J Mater Sci (2014) 49:1279–1285
DOI 10.1007/s10853-013-7811-x

Study of the relationship between crystal structure and luminescence in rare-earth-implanted Ga_2O_3 nanowires during annealing treatments

I. López · K. Lorenz · E. Nogales · B. Méndez · J. Piqueras · E. Alves · J. A. García

Received: 21 June 2013 / Accepted: 30 July 2013 / Published online: 22 October 2013

Abstract A systematical analysis of the correlation between the crystalline quality and the luminescence of rare-earth-implanted β-Ga_2O_3 nanostructures with potential applications in visible and ultraviolet photonics is presented. Europium ions led to red emission while gadolinium ions are efficient ultraviolet emitters. Different degrees of lattice recoveries of the nanostructures have been achieved after implantation by rapid thermal annealing treatments carried out at different temperatures. The recovery process has been analyzed by transmission electron microscopy (TEM), high-resolution TEM, and Raman techniques. High-fluence implantation with either of the two rare earth ions induces partial amorphization of the structures. Partial recrystallization of the nanostructures above 500 °C is revealed by Raman analysis. Nearly complete recovery of the crystal structure is obtained in the annealing temperature range 900–1100 °C, coincident with the expected value for bulk Ga_2O_3. Cathodoluminescence and photoluminescence allowed comparison of the Eu^{3+} and Gd^{3+} intraionic luminescence lines after annealing at different temperatures and their correlation with the crystallinity. It has been found that the width of the Eu^{3+} luminescence lines clearly correlates with the width of the Raman peaks, both decreasing with annealing temperature, which shows the possibility of using the luminescence of this rare earth as a probe for lattice disorder. On the other hand, our results suggest that Gd^{3+} lines are much less sensitive to disorder.

I. López · E. Nogales (✉) · B. Méndez · J. Piqueras
Departamento de Física de Materiales, Universidad Complutense de Madrid, 28040 Madrid, Spain
e-mail: emilio.nogales@fis.ucm.es

K. Lorenz · E. Alves
IST/ITN, Instituto Superior Técnico, Estrada Nacional 10, 2686-953 Sacavém, Portugal

J. A. García
Departamento de Física Aplicada II, Universidad del País Vasco, Apdo. 644, 48080 Bilbao, Spain

Introduction

Ion implantation is a routinely used technique to accurately dope semiconductor wafers in microelectronic industry, with the aim of modifying electrical conductivity, as for example to obtain n-type or p-type conductivity [1]. To the same extent, optical properties such as luminescence may be tuned by rare earth ion implantation of semiconductors or insulators [2, 3]. The main advantages of ion implantation for doping purposes are twofold: the possibility to dope very small areas and the achievement of an effective and controlled doping with ions that show very low diffusivity coefficients. In particular, rare earth ions usually show very low diffusivity in semiconductor hosts and this issue is tightened in nanowire targets [1]. On the other hand, the lattice damage generated by ion bombardment generally becomes the main drawback, because of the resulting luminescence degradation. However, this issue is usually overcome by specific annealing processes. In particular, rapid thermal annealing (RTA) is very convenient and cost-effective compared to longer thermal treatments. Ion implantation, in particular rare earth implantation of nanowires has not been explored widely [1, 4–7]. Hence, there is still work to do concerning the investigation of the crystal lattice damage and the way to optimize the activation of luminescence of RE ions in nanowires via thermal treatments.

In this work, gallium oxide nanowires have been doped with Gd^{3+} and Eu^{3+} ions by implantation and RTA treatments. The crystalline properties of the as-implanted and rapid thermal annealed Ga_2O_3 nanowires at different temperatures have been studied by transmission electron microscopy (TEM) and Raman. Luminescence properties of the as-implanted and post-annealed nanowires were investigated by photoluminescence (PL) or cathodoluminescence (CL) techniques. Conditions for lattice recovery accompanying activation of luminescence centers are discussed.

Experimental

Undoped Ga_2O_3 nanowires have been synthesized by a thermal evaporation method from a metallic gallium source. The thermal treatment was conducted at 1100 °C during 10 h in an open furnace. Large quantity of Ga_2O_3 nanowires, with lateral dimensions between a few tens of nanometers and several microns and lengths up to tens of microns, grew on the surface of a compacted gallium oxide pellet used as substrate, as shown elsewhere [6]. The nanowires were detached and placed onto pieces of silicon wafers for the implantation process of Eu^{3+} or Gd^{3+} ions. The ions were implanted at 150 keV with a fluence of 5×10^{15} cm^{-2}. Due to the distribution of the nanowires on the substrate, see Ref. [6], the ion implantation does not produce a uniform doping in all of them. After the implantation, a RTA process was carried out using a halogen lamp furnace by Annealsys for 30 s under Ar flow (1 atm) conditions for lattice recovery on four different samples, each of them at a different temperature: 500, 700, 900, and 1100 °C. The study of the structural and luminescence properties was performed in both the as-implanted and the set of post-implanted RTA Ga_2O_3 nanowires.

Morphological characterization has been carried out in a Leica Stereoscan 440 scanning electron microscope (SEM). TEM, selected area electron diffraction (SAED), and high-resolution TEM (HRTEM) were performed in a JEOL JEM 200 electron microscope. CL measurements were carried out in the above-mentioned Leica SEM or a Hitachi S2500 SEM. PL spectroscopy studies were performed by exciting with an optical parametric oscillator (OPO) laser Ekspla 342B, tuned at 248.0 nm (±0.1 nm) and acquiring the luminescence signal with an Edinburgh Instruments CD900 spectrometer at 10 K using a closed cycle liquid He system. Spatially resolved Raman spectroscopy has been done in a Horiba Jobin–Yvon LabRam HR800 Raman confocal microscope. The excitation light was the 325 nm line of a HeCd laser. The study of the structures was complemented with the aid of high-resolution X-ray photoemission spectra and imaging, performed at the Sincrotrone Elettra Trieste facility (ESCA-microscopy line).

Results and discussion

In order to systematically assess the recovery of the crystalline quality by thermal annealing, Raman analysis in a confocal microscope has been carried out for the samples annealed at different temperatures. Raman spectra from individual Eu-implanted Ga_2O_3 elongated nanostructures, both not annealed and annealed at 500, 700, 900, or 1100 °C, are shown in Fig. 1a. All these structures had thicknesses in the range of tens of nanometers, so that their whole volume was implanted. For comparison, the Raman spectrum corresponding to undoped Ga_2O_3 nanowires is also shown. A clear evolution of the Raman spectra with annealing temperature is observed.

For the as-implanted wires, as well as those annealed at 500 °C, spectra show broad peaks which indicates a low crystalline quality and even amorphization, as discussed below for TEM results. For the wires annealed at 700 °C sharp peaks are observed, but with a higher FWHM than those of the as-grown sample. This shows that the recovery starts in the 500–700 °C temperature range. However, at 700 °C the crystalline quality is not yet fully recovered. It is well known that the linewidths increase when the material is damaged or disordered, due to phonon damping or changes in the rules for momentum conservation in the Raman process [8, 9]. On the other hand, at 900 °C the spectra show peaks with FWHM very similar to those of the reference, as-grown nanowire. Although a good recovery is reached at this annealing temperature, still some peaks are somewhat wider than those of the reference undoped Ga_2O_3 nanowire, especially those related to octahedron modes, i.e., the 350 and 415 cm^{-1} peaks [10]. Finally, annealing at 1100 °C yields Raman peaks which are virtually equal to those from the as-grown sample. Similar results are obtained for Gd-implanted nanowires (Fig. 1b). This is expected, due to the fact that the two ions are neighbors in the periodic table, having very similar masses (atomic weight for Eu = 152.0, atomic weight for Gd = 157.3). Ion implantation simulations obtained with the SRIM package [11] for both Gd and Eu yield almost identical profiles as shown in Fig. 2, with peak concentration of about 10^{21} cm^{-3} at about 30 nm depth. The damage is produced in the volume where the ions have penetrated, which reaches a depth of about 80 nm below the surface. For this reason, the damage created during implantation and, in general, the structural properties studied for one ion can be extended to the other one. The simulations are performed for a flat surface geometry and do not take into account the surface curvature of the

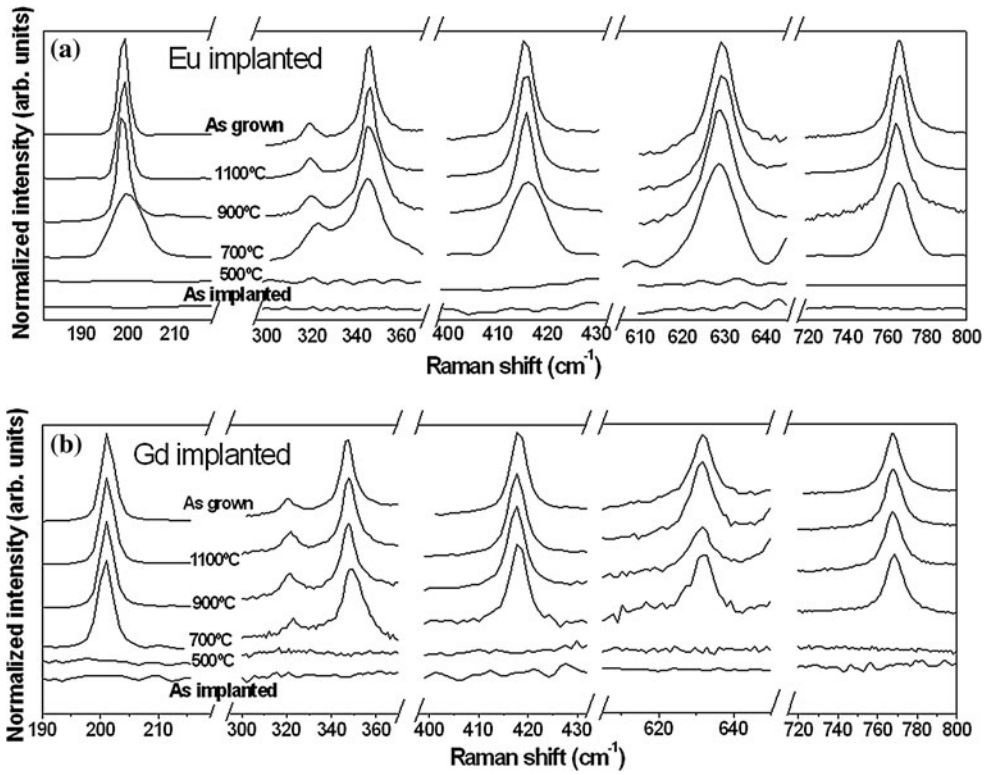

Fig. 1 **a** Raman spectra from: an as-grown monocrystalline nanowire (*top spectrum*), and Eu-implanted nanowires which were as-implanted (*bottom spectrum*), or annealed at 500, 700, 900, or 1100 °C. **b** Raman results from Gd-implanted nanowires. The peak intensities are normalized and shifted vertically for clarity

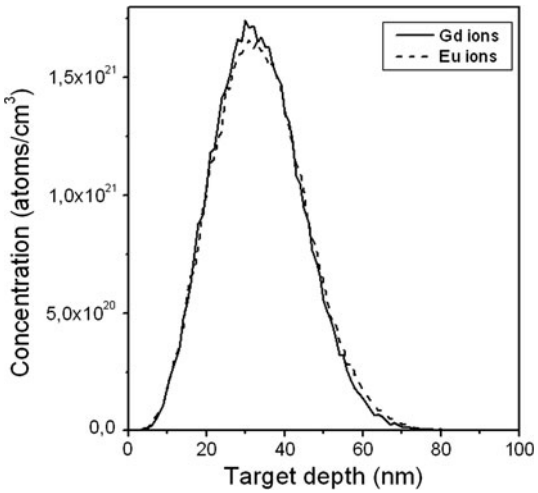

Fig. 2 Ion concentration profile obtained with SRIM simulation for the Eu (*dashed line*) and Gd (*solid line*) implantation conditions used in this work in gallium oxide. Almost identical profiles are obtained for both ions

nanowires. Nevertheless, the conclusion that the properties studied for one ion can be extended to the other one is valid, independent of the geometry, and the penetration depth we have obtained can be considered as a good qualitative estimation for the nanowires.

The annealing temperatures have been chosen according to the expected structural reparation and optical activation of RE ions in bulk or thin film matrices. The accepted general rule is that an annealing temperature of about 2/3 of the melting temperature (in Kelvin) of the implanted bulk material is needed to get full recovery of the crystallinity after ion implantation [1]. For β-Ga_2O_3, the melting temperature is around 1800 °C (about 2070 K). Therefore, the full crystalline recovery for bulk gallium oxide is expected to be achieved at about 1100 °C (about 1380 K), which is very close to the value inferred for the nanowires from these results.

It was shown in a previous work [6] that the nanowire morphology is not modified during ion implantation with Eu or Gd, or after the subsequent annealing treatments.

TEM analysis was performed on Gd^{3+}-implanted Ga_2O_3 nanowires. The results are shown in Fig. 3. Figure 3a shows the SAED pattern corresponding to an as-implanted structure and reveals clear amorphization of the structure, although some diffraction spots are observed due to the presence of crystalline regions. This is in accordance with the Raman results shown in Fig. 1. Strongly ionic semiconductors, such as ZnO, cannot be completely amorphized, even for very high fluences of heavy ions as those used in the present work [1, 5]. Monoclinic gallium oxide

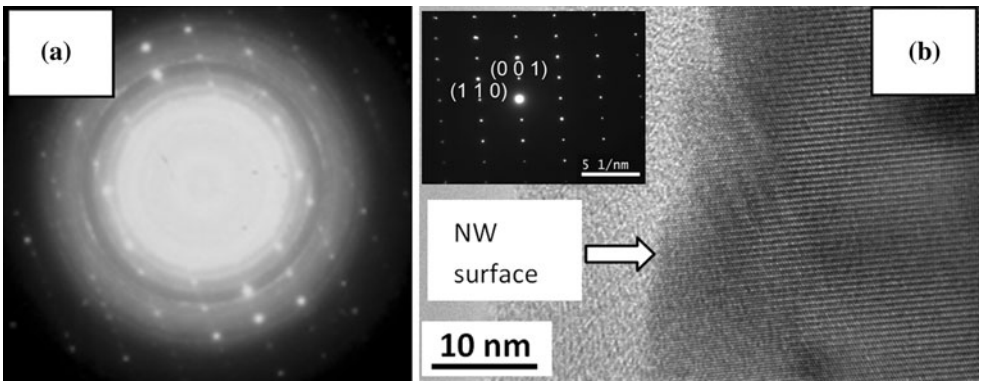

Fig. 3 **a** SAED pattern of a Gd as-implanted nanostructure. **b** HRTEM image of a nanostructure implanted with Gd and annealed at 1100 °C. The *inset* shows the SAED pattern, showing a [110] zone axis

presents a lower degree of ionicity than ZnO, which explains the observed degree of amorphization [12]. Figure 3b shows the HRTEM image of a structure that was annealed at 1100 °C after ion implantation. Even though extended defects can still be found, the crystalline quality was mostly recovered, which is further confirmed by the corresponding SAED pattern indexed according to the monoclinic β-Ga_2O_3 structure (inset in Fig. 3b).

Spatially resolved XPS results from Eu-implanted Ga_2O_3 nanowires are presented in Fig. 4, in order to assess the possible influence of the implantation damage on the local electronic features of the different elements.

Maps of the Ga 3d line signal for two Eu-implanted Ga_2O_3 nanowires, one as-implanted and one implanted and annealed at 900 °C, are shown in Fig. 4a, b, respectively. They have cross sections around 900 and 650 nm, respectively, which ensures that the probe diameter, around 200 nm, generated the signal only from the wires and not from the surrounding Si substrate. Local XPS spectra from these two nanowires are shown in Fig. 4c in the valence band range. The 4f Eu core level is observed at around 3.4 eV from the Fermi level. Figure 4d–i show the Ga 3d, O 1s, and Eu 4d peaks of these two structures. The corresponding spectra from an as-grown nanowire are shown for comparison in Fig. 4j, k. All XPS spectra were calibrated with the C 1s binding energy (BE) at 284.8 eV [13]. Deconvolution of the Ga 3d peaks is virtually the same for the two implanted samples with three peaks at about 19.0, 19.9, and 20.8 eV. The peak at around 20.8 eV is assigned to Ga in Ga_2O_3 [14]. The 19.0 eV peak has been previously assigned to an unidentified impurity (possibly metallic Ga clusters) [14, 15] while the peak at around 19.9 eV is assigned to another impurity, possibly Ga–O–OH species [14]. For the as-grown Ga_2O_3 nanowire, the deconvolution yields peaks positions at 19.0, 20.0, and 20.6 eV. Therefore, the Ga 3d peak presents in the implanted samples very similar features as in the reference one. However, a slight shift of about 0.2 eV of the peak corresponding to Ga in Ga_2O_3 is observed after implantation, which could be related to some defects of the nanowires (see TEM image in Fig. 3).

More significant changes are observed for the O 1 s peak in the implanted samples. In the as-grown nanowire the O 1s line is composed by two peaks at 531.9 and 532.5 eV (Fig. 4k). For metal oxides, the lower BE component is usually assigned to the oxide (i.e., Ga–O–Ga bonds). The higher BE component is usually assigned to species such as hydroxides and adsorbed oxygen [16, 17]. For the implanted samples, before and after annealing, the higher energy peak related to hydroxides is slightly shifted to 532.8 eV. Also, an additional peak is observed at 533.8 eV, which could be related to oxygen bonded to europium and gallium, although the energy shift is too high. Alternatively, the presence of the silicon wafer during implantation and annealing could be responsible for some Si deposited on the surface of the nanowires due to sputtering during the implantation, which could explain this higher energy peak. Indeed, the BE for oxygen in SiO_2 is in the range 533–534.3 eV [14].

Finally, two peaks corresponding to europium, at 129.0 and 135.0 eV, are observed in Fig. 4f, i. The energy position correlates well to the peaks observed for Eu^{3+} in Eu_2O_3. In principle, the position should not be very sensitive to a change into a Ga_2O_3 environment. The lower energy peak is the shake-down satellite, as previously observed for different compounds [18].

In order to get insight into the luminescence improvement of the nanostructures, as well as its correlation with the structural recovery during thermal annealing, CL analysis was performed at room temperature for the Eu-implanted sample series (Fig. 5). The spectra of Fig. 5 correspond to nanowires annealed at different temperatures. The spectrum for the as-implanted nanowires is also shown for comparison (top spectrum). The emission consists of the characteristic peaks due to the ^5D_i–^7F_j ($i = 0, 1, 2$ and $j = 0, 1, 2, 3, 4$) intraionic transitions of the Eu^{3+}

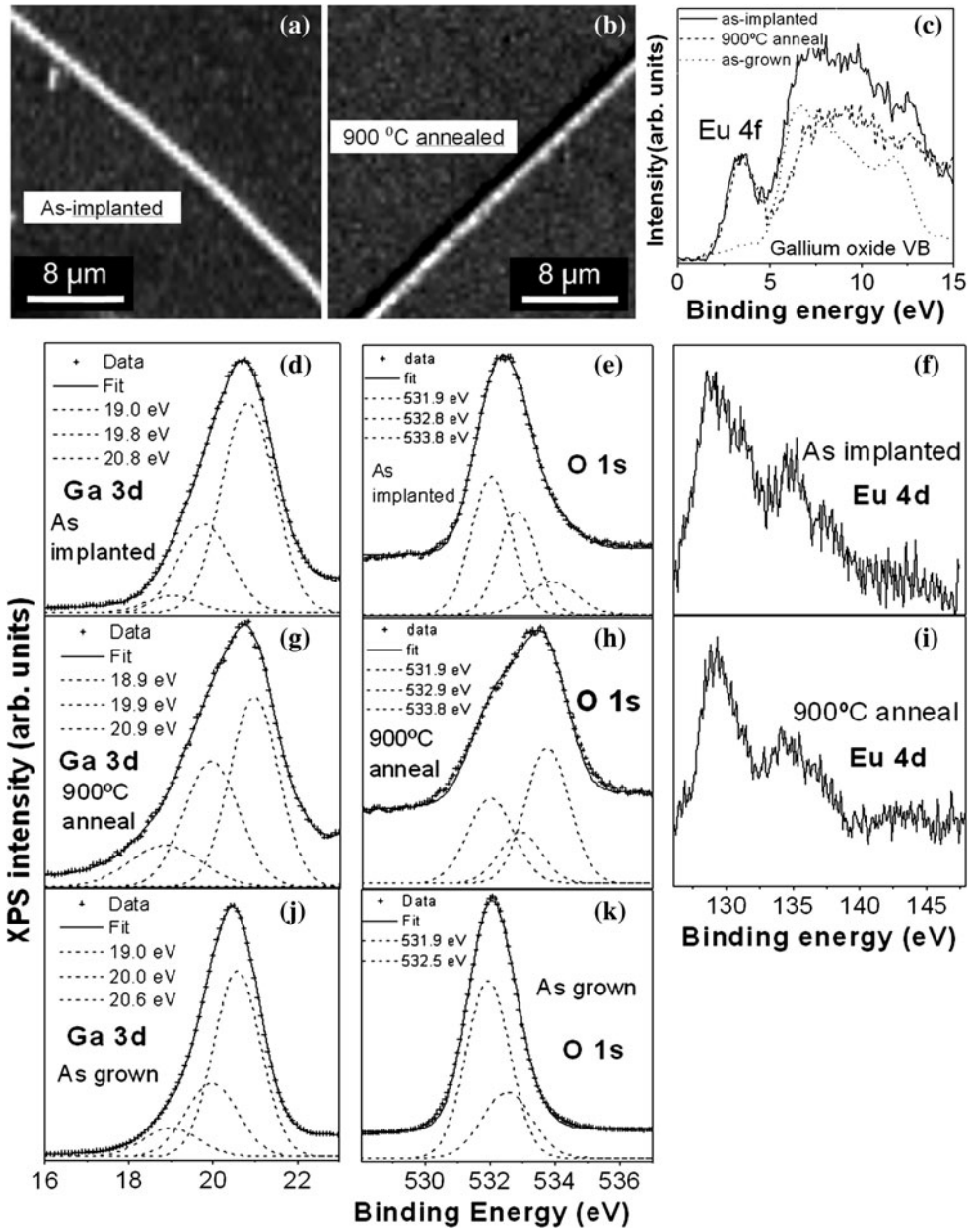

Fig. 4 XPS results for Eu-implanted samples. **a** XPS map of the Ga 3d line from an as-implanted nanowire **b** XPS map of the Ga 3d line from an implanted and 900 °C annealed nanowire. Local XPS spectra from these nanowires are shown in figures (**c**)–(**i**) for valence band, Ga 3d, O 1s, and Eu 4d. Spectra for valence band, Ga 3d and O 1s from a reference, as-grown nanowire are also shown in (**c**), (**j**), and (**k**), respectively

ions. The most intense corresponds to the $^5D_0$–$^7F_2$ transition, at 610 nm. Luminescence is obtained even without annealing, which was already pointed out in a previous study [6]. Besides, a clear evolution is observed with the annealing temperature: the peaks get sharper by increasing temperature up to 900 °C. At 1100 °C, the peaks look very similar to those after annealing at 900 °C. This sharpening of the peaks is explained by the damage recovery after annealing: the rare earth energy levels are slightly sensitive to the local crystal symmetry [19]; therefore, high implantation damage results in an inhomogeneous broadening of the emission lines. Hence, the better is the damage recovery the more homogeneous is the symmetry for most of the emitting centers, which results in sharper luminescence lines.

These CL results agree with the Raman results (Fig. 1), in which the crystallinity was found to be almost completely recovered after the 900 °C annealing. This suggests the use of the Eu^{3+} luminescence as a nanoscopic probe of the crystalline quality of the implanted nanostructures. The

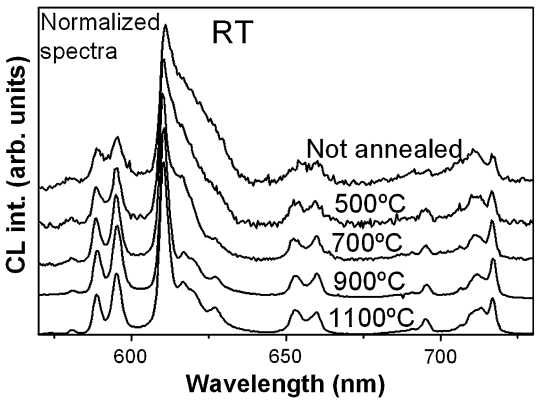

Fig. 5 Room-temperature CL spectra from the as-implanted and annealed Eu-implanted samples for annealing at different temperatures

Eu^{3+} luminescence lines could be used for characterization of lattice disorder in a different case if the ions had their origin in a different method than ion implantation, e.g., incorporation of Eu^{3+} during the growth of the nanowires. Otherwise, the damage induced by ion implantation would severely modify what had to be characterized.

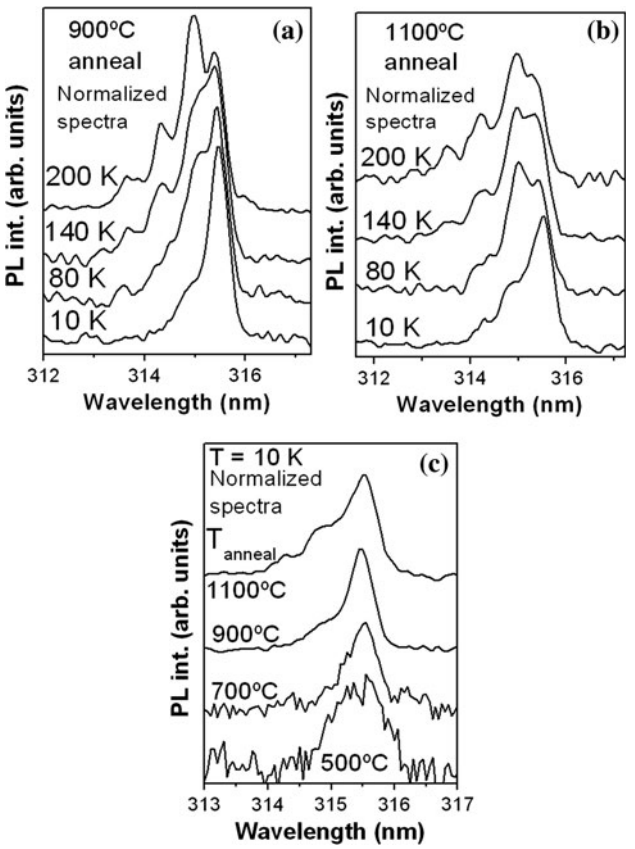

Fig. 6 **a** PL spectra acquired at different temperatures from Gd-implanted nanowires annealed at 900 °C. **b** PL spectra acquired at different temperatures from nanowires annealed at 1100 °C. **c** PL spectra acquired at $T = 10$ K from samples annealed at 500, 700, 900, and 1100 °C. All spectra are normalized. $\lambda_{exc} = 248$ nm

CL spectra from Gd-implanted nanowires did not allow a comparison of the luminescence peaks of the different samples due to the very low emission after annealing at 500 and 700 °C. In order to make this comparison, PL analysis of these samples was performed at different temperatures. The resulting spectra are shown in Fig. 6, in the region of the characteristic $^6P_{7/2}$–$^8S_{7/2}$ Gd^{3+} related luminescence peak. Figure 6a, b show the spectra acquired at different temperatures for the samples annealed at 900 and 1100 °C. They show several sharp lines, as previously observed for Gd^{3+} in AlN, in which the lines were assigned to individual components belonging to the $^6P_{7/2}$ multiplet, because of the Stark splitting [20, 21]. As the measurement temperature increases, the relative intensity of the higher energy (lower wavelength) lines increases. This is expected, due to the fractional thermal population of higher energy levels.

The evolution of the PL peaks as the RTA temperature increases is analyzed in Fig. 6c. For the case of the as-implanted sample, the luminescence peak could not be observed. For the annealed samples, a similar analysis of the line width as that performed with the CL in Eu-implanted samples is difficult to achieve. The obtained results suggest that these Gd^{3+} levels have a much lower sensitivity to disorder in comparison with the Eu^{3+} levels.

Conclusions

We have systematically studied the effective doping of β-Ga_2O_3 nanostructures with Eu^{3+} and Gd^{3+} by ion implantation for potential applications in visible and ultraviolet photonics. The crystal recovery of the nanostructures has been analyzed as a function of the annealing temperature during RTA treatments subsequent to ion implantation. Both TEM and Raman show amorphization of the structures after high-fluence implantation with both ions. Raman analysis shows a slight recrystallization of the nanostructures above 500 °C and a nearly complete recovery of the crystallinity in the annealing temperature range 900–1100 °C, which is confirmed by TEM. This value is the expected one for this material. The behavior of the luminescence of the nanostructures has been studied by CL in the case of Eu-implanted nanowires and PL in the case of Gd implantation. CL analysis of the Eu-implanted samples show a clear correlation between the line broadening of the Eu luminescence lines and the Raman lines, suggesting the possibility of using the luminescence of this rare earth as a probe for lattice disorder. PL analysis of Gd^{3+} lines has shown that they are much less sensitive to disorder than the Eu^{3+} lines.

Acknowledgements This work has been supported by MICINN through Project MAT 2012-31959, and Consolider CSD 2009-00013. The authors are grateful to Dr. Luca Gregoratti at the Sincrotrone Elettra Trieste for useful advice on XPS measurements. We thank Sérgio Miranda (IST/ITN) for the RTA treatments. Financial support by FCT Portugal is acknowledged (PTDC/CTM/100756/2008; PTDC/CTM-NAN/2156/2012).

References

1. Ronning C, Borschel C, Geburt S, Niepelt R (2010) Mat Sci Eng R 70:30
2. Steckl AJ, Park JH, Zavada JM (2007) Mater Today 10:20
3. Lorenz K, Alves E, Gloux F, Ruterana P (2010) In: O'Donnell KP, Dierolf V (eds) Rare earth doped III-nitrides for optoelectronic and spintronic applications. Springer, Dordrecht
4. Wang J, Hark SK, Li Q (2006) Microsc Microanal 12:748
5. Geburt S, Stichtenoth D, Mueller S, Dewald W, Ronning C, Wang J, Jiao Y, Rao YY, Hark SK, Li Q (2008) J Nanosci Nanotechnol 8:244
6. Nogales E, Hidalgo P, Lorenz K, Méndez B, Piqueras J, Alves E (2012) Nanotechnology 22:285706
7. Nogales E, López I, Méndez B, Piqueras J, Lorenz K, Alves E, García JA (2012) Proc SPIE 8263:82630B
8. Perkowitz S (1993) Optical characterization of semiconductors: infrared, Raman and photoluminescence spectroscopy. Academic Press, Cambridge
9. Gouadec G, Colombam P (2007) Progr Cryst Growth Charact Mater 53:1
10. Dohy D, Lucazeau G, Revcolevschi A (1982) J Sol State Chem 45:180
11. Ziegler JF, Biersack JP and Ziegler MD. SRIM 2008 - The Stopping and Range of Ions in Matter, SRIM Co., Chester, http://www.srim.org/ (last accessed April 2013)
12. Zhuravlev VD (2007) Bull Russ Acad Sci 71:681
13. Miller DJ, Biesinger MC, McIntyre NS (2002) Surf Interface Anal 33:299
14. NIST Standard Reference Database 20, Version 4.1. Alexander V. Naumkin, Anna Kraut-Vass, Stephen W. Gaarenstroom, and Cedric J. Powell, http://srdata.nist.gov/xps (last accessed April 2013)
15. Ghosh SC, Biesinger MC, LaPierre RR, Kruse P (2007) J Appl Phys 101:114322
16. López I, Utrilla AD, Nogales E, Méndez B, Piqueras J, Peche A, Ramírez-Castellanos J, González-Calbet JM (2012) J Phys Chem C 116:3935
17. Al-Kuhaili MF, Durrani SMA, Khawaja EE (2003) Appl Phys Lett 83:4533
18. Mercier F, Alliot C, Bion L, Thromat N, Toulhoat P (2006) J Electron Spectrosc Relat Phenom 150:21
19. Dierolf V, Sandmann C, Zavada J, Chow P, Hertog B (2004) J Appl Phys 95:5464
20. Vetter U, Zenneck J, Hofsäss H (2003) App Phys Lett 83:2145
21. Kitayama S, Yoshitomi H, Iwahashi S, Nakamura J, Kita T, Chigi Y, Nishimoto T, Tanaka H, Kobayashi M, Ishihara T, Izumi H (2011) J Appl Phys 110:093108